New Rate-2 STBC Design for 2 TX with Reduced-Complexity Maximum Likelihood Decoding

Payam Rabiei, *Student Member, IEEE*, Naofal Al-Dhahir, *Fellow, IEEE* and Robert Calderbank, *Fellow, IEEE*

***Abstract*—We propose a new full-rate space-time block code (STBC) for two transmit antennas which can be designed to achieve maximum diversity or maximum capacity while enjoying optimized coding gain and reduced-complexity maximum-likelihood (ML) decoding. The maximum transmit diversity (MTD) construction provides a diversity order of $2N_r$ for any number of receive antennas N_r at the cost of channel capacity loss. The maximum channel capacity (MCC) construction preserves the mutual information between the transmit and the received vectors while sacrificing diversity. The system designer can switch between the two constructions through a simple parameter change based on the operating signal-to-noise ratio (SNR), signal constellation size and number of receive antennas. Thanks to their special algebraic structure, both constructions enjoy low-complexity ML decoding proportional to the square of the signal constellation size making them attractive alternatives to existing full-diversity full-rate STBCs in [6], [3] which have high ML decoding complexity proportional to the fourth order of the signal constellation size. Furthermore, we design a differential transmission scheme for our proposed STBC, derive the exact ML differential decoding rule, and compare its performance with competitive schemes. Finally, we investigate transceiver design and performance of our proposed STBC in spatial multiple-access scenarios and over frequency-selective channels.**

***Index Terms*—Diversity, MIMO, space-time block codes, single-carrier frequency-domain equalization.**

I. Introduction

THE Vertical Bell Labs layered space-time (V-BLAST) architecture, proposed in [7], is a well-known multi-input multi-output (MIMO) system which operates at very high spectral efficiency with low encoding and decoding complexities. However, V-BLAST can not exploit the maximum diversity available in a MIMO channel and, therefore, can suffer appreciable performance loss.

Orthogonal STBCs (OSTBC) [1] [2], on the other hand, are primarily designed to capture full transmit diversity of the MIMO channel while keeping the decoding complexity linear in the number of transmit antennas. Due to their orthogonal structure constraint, OSTBC suffers from rate loss, e.g. the Alamouti scheme transmits 1 symbol per channel use which is only half the maximum rate possible with two transmit antennas. Moreover, with the exception of the Alamouti STBC with 1 receive antenna [1], OSTBC schemes do not preserve the mutual information [17] between the received and the transmit signal vectors due to the induced space-time correlation on the channel matrix.

These observations motivated researches to design several STBCs for $N_t = 2$ which not only achieve the capacity of the underlying MIMO channel but also ensure maximum diversity, thanks to their special algebraic structure. A number-theoretic STBC construction, called $B_{2,\phi}$, was proposed in [3] and proved to be a full-diversity capacity-achieving STBC. For more than one receive antenna, the performance of $B_{2,\phi}$ was shown to be superior to the Alamouti STBC at the same rate. Following the pioneering work of Damen *et al*, three approaches that achieve the optimum diversity-multiplexing gain tradeoff were proposed independently in [4], [5] and [6]. The schemes in [6] and [4] were shown to be identical (related by an invertible transformation), have optimum coding gain, and outperform the one in [3]. However, the main drawback of the schemes in [3], [4] and [6] is the exponentially-growing ML decoding complexity as a function of the number of transmit antennas and constellation size.

In this paper, we derive a new STBC design for $N_t = 2$ transmit antennas and $t = 2$ time slots which enjoys low-complexity ML decoding (quadratic in the constellation size) with comparable performance with respect to the previous full-diversity full-rate (FDFR) codes in [3], [4], [5], [6]. We reduce the ML decoding complexity by exploiting the algebraic structure of the code using a hybrid maximum-likelihood interference cancellation (HMLIC) decoding algorithm which we show to be ML optimal.

Our proposed code can be represented as a linear combination of two Alamouti codes and does not achieve the optimum diversity-multiplexing tradeoff. However, by optimizing the linear combination coefficients, we present maximum-diversity and maximum-capacity constructions of the code, maximize the coding gain, and analyze their properties. Several applications of the proposed STBC design are investigated including differential transmission, multi-user transmission using spatial division multiple access, and broadband transmission over frequency-selective channels.

Related code constructions were developed independently in [8]- [13]. We have compared the coding gain achieved by some of these codes with our code in Table I. As we

Manuscript received January 2, 2008; revised May 16, 2008, September 5, 2008, and November 1, 2008; accepted November 15, 2008. The associate editor coordinating the review of this paper and approving it for publication was A. Chockalingam.

This work was supported in part by the National Science Foundation (NSF) under contracts CCF 04-30654 and by a gift from Texas Instruments Inc.

P. Rabiei and N. Al-Dhahir are with the Department of Electrical Engineering and Computer Science, University of Texas at Dallas (e-mail: payam@utdallas.edu).

R. Calderbank is with the Department of Electrical Engineering, Princeton University.

Digital Object Identifier 10.1109/T-WC.2009.071323

TABLE I
CODING GAIN COMPARISON FOR DIFFERENT CONSTELLATION SIZES

	4bpcu, $\theta = \tan^{-1}(0.5)$	8bpcu, $\theta = \tan^{-1}(0.25)$
Golden [6]	1.7889	1.7889
$B_{2,\phi}$ [3]	0.2369	0.0591
Varanasi [4]	1.7889	1.7889
Sari [10]	$\sqrt{2}$	$\sqrt{2}$
MTD	0.8	0.2353

will show in Section VIII (c.f. Fig.4), these codes achieve comparable performance to our proposed code at similar or higher decoding complexity. In addition, we optimize our code design analytically, develop its non-coherent (differential) encoding/decoding scheme, and generalize it to frequency-selective and multiple-access channels. All of these issues were not considered in [8], [9], [10] and [13].

The rest of this paper is organized as follows. In Section II, we describe the system model and briefly review the code design criteria. In Section III, we present the code design procedure and analyze its achievable diversity order and mutual information. In Section IV, we present a reduced-complexity ML decoding algorithm in Rayleigh flat-fading channels while in Section V, we design the differential encoder and the differential ML decoder. In Sections VI and VII we show how to apply our code to multiple-access and frequency-selective channels. Simulation results are presented in Section VIII and the paper is concluded in Section IX.

II. SYSTEM MODEL AND DESIGN CRITERIA

Consider a vector of 4 information symbols, $\boldsymbol{s} = [s_1\ s_2\ s_3\ s_4]^T$ where $[\cdot]^T$ denotes the matrix transpose and the information symbols $s_j, j = 1, \cdots, 4$, belong to a q-QAM constellation and transmitted from $N_t = 2$ antennas during $t = 2$ symbol periods. Define an $N_t \times t$ matrix $\boldsymbol{u}(\boldsymbol{s})$ as the STBC codeword associated with the vector $\boldsymbol{s}$ with the entries $u_{m\nu}$ which is transmitted from $m = 1, \cdots, N_t$ antennas over symbol periods $\nu = 1, \cdots, t$. The received signal matrix of size $(N_r \times t)$ is given by

$$\boldsymbol{y} = \sqrt{\frac{\rho}{N_t}}\boldsymbol{H}\boldsymbol{u} + \boldsymbol{w} \qquad (1)$$

where $\boldsymbol{H} \in \mathbb{C}^{N_r \times N_t}$ denotes the channel matrix with entries h_{rm} representing the fading coefficients associated with the mth transmit and the rth receive antenna. The channel coefficients are samples of an independent and identically distributed (i.i.d.) complex Gaussian random process with zero mean and variance 0.5 per real dimension. The channel coefficients are assumed quasi-static flat-fading i.e. fixed during one STBC transmission of t symbol periods. The noise matrix $\boldsymbol{w} \in \mathbb{C}^{N_r \times t}$ has entries $w_{r\nu}$ which are drawn from a white Gaussian distribution $\mathcal{CN}(0, \sigma^2)$. The received signal matrix $\boldsymbol{y} \in \mathbb{C}^{N_r \times t}$ is generated by stacking signal samples from the N_r receive antennas at time slots $1, \cdots, t$. The normalization factor $\sqrt{\frac{\rho}{N_t}}$ in (1) ensures that ρ is the SNR at each receive antenna since $\mathsf{E}[tr\{\boldsymbol{u}\boldsymbol{u}^*\}] = N_t$ where $\mathsf{E}[\cdot]$ and $tr\{\cdot\}$ are the expectation and trace operations, respectively. Since it takes t time slots (number of columns of $\boldsymbol{u}$) to transmit p symbols (size of the vector $\boldsymbol{s}$), the transmission rate is defined as

$$\mathcal{R}_s = \frac{p}{t}\log_2 q \quad : \quad \text{bits per channel use (bpcu)} \qquad (2)$$

where q is the cardinality of the signal constellation used. Note that an STBC is said to be full-rate if $\mathcal{R}_s^{\max} = N_t$ symbols pcu.

III. PROPOSED 2×2 STBC DESIGN

A. Maximum Transmit Diversity (MTD) Construction

Divide the information symbols in $\boldsymbol{s} = [s_1\ s_2\ s_3\ s_4]^T$ into two groups, each of which consists of two information symbols. The symbols of the first group $s_i^{'}$ are obtained through a complex rotation applied to the original symbols i.e. $s_i^{'} = s_i e^{j\omega}, i = 1, 2$ where ω is chosen as a function of the signal constellation. Multiplying the symbols in the first group by $e^{j\omega}$ provides the so-called "signal space diversity" [1]. Next, we encode each group with an Alamouti encoder i.e.

$$\mathcal{G}_1 : [s_1^{'}, s_2^{'}] \mapsto \begin{bmatrix} s_1^{'} & s_2^{'} \\ -s_2^{'*} & s_1^{'*} \end{bmatrix} = \begin{bmatrix} \mathcal{V}_1^{'} & \mathcal{V}_2^{'} \end{bmatrix} \qquad (3)$$

$$\mathcal{G}_2 : [s_3, s_4] \mapsto \begin{bmatrix} s_3 & s_4 \\ -s_4^{*} & s_3^{*} \end{bmatrix} = \begin{bmatrix} \mathcal{V}_1 & \mathcal{V}_2 \end{bmatrix} \qquad (4)$$

where $\mathcal{V}_i^{'}$ for $i = 1, 2$ represents the ith column of the Alamouti code in (3). Similarly, $\mathcal{V}_j, j = 1, 2$ is the jth column of the Alamouti code in (4).

Construction Procedure:

Defining the real-valued matrix [2] $\boldsymbol{R} \triangleq \begin{bmatrix} \alpha_1 & \beta_1 \\ \alpha_2 & \beta_2 \end{bmatrix}$, we generate the MTD STBC codeword as follows

$$\boldsymbol{u} \triangleq \text{diag}\left(\boldsymbol{R}\begin{bmatrix} \mathcal{V}_1^{'} & \mathcal{V}_2^{'} \end{bmatrix}\right) + \text{diag}\left(\boldsymbol{R}\begin{bmatrix} \mathcal{V}_1 & \mathcal{V}_2 \end{bmatrix} J\right) J \qquad (5)$$

where the diag$(\cdot)$ operator constructs a diagonal matrix by setting the off-diagonal elements to zero and $J = \begin{bmatrix} 0 & 1 \\ 1 & 0 \end{bmatrix}$ is the reversal matrix. Substituting from (3) and (4) into (5) we get

$$\boldsymbol{u} = \begin{bmatrix} s_1^{'}\alpha_1 - s_2^{'*}\beta_1 & s_3^{*}\beta_1 + s_4\alpha_1 \\ s_3\alpha_2 - s_4^{*}\beta_2 & s_1^{'*}\beta_2 + s_2^{'}\alpha_2 \end{bmatrix} \qquad (6)$$

The matrix $\boldsymbol{R}$ is designed to maximize the coding gain and guarantee full diversity of the proposed MTD code in (6) as follows

$$\Psi_\theta = \underset{\substack{\theta_1, \theta_2 \in [0, \pi/2] \\ \boldsymbol{s}_1 \neq \boldsymbol{s}_2}}{\arg \max} \{G_c\} \qquad (7)$$

where

$$G_c = \min_{\boldsymbol{s}_1 \neq \boldsymbol{s}_2} \|\det\left[\boldsymbol{u}(\boldsymbol{s}_1) - \boldsymbol{u}(\boldsymbol{s}_2)\right]\| \neq 0 \qquad (8)$$

The angles θ_1 and θ_2 in (7) are related to α_1, α_2, β_1 and β_2 by the following relations

$$\alpha_1 = \sin(\theta_1); \beta_1 = \cos(\theta_1); \alpha_2 = \sin(\theta_2); \beta_2 = \cos(\theta_2) \qquad (9)$$

These definitions ensure that there is no transmit energy increase due to STBC encoding, i.e. $\alpha_1^2 + \beta_1^2 = 1$ and similarly

[1] Using computer search to maximize coding gain, we found that the best rotation angle for 4-QAM is $\omega = \pi/4$.

[2] To simplify the analysis, we consider only a real-valued $\boldsymbol{R}$. However, our design procedure can be generalized to a complex-valued $\boldsymbol{R}$ as well.

$\alpha_2^2 + \beta_2^2 = 1$.

Proposition 1:
Subject to the constraint that $\theta_1 + \theta_2 = \pi/2$, the solution to the code design problem in (7) for the 4-QAM constellation is given by

$$\{\theta_1^{\text{opt}}, \theta_2^{\text{opt}}\} = \{\arctan(2), \arctan(\frac{1}{2})\} \quad (10)$$

Proof: See Appendix I. ■

Remarks:

1. Our proposed STBC in (6) has the property that the average transmitted power is equal to the average original signal constellation power, i.e. the power required to transmit the linear combination of the information symbols equals the power required to transmit the symbols individually. It also induces a uniform average transmitted power per antenna in all time slots, i.e., all entries in the codeword have the same average power.

2. The same procedure can be followed to optimize θ_1 and θ_2 for other signal constellations. For example, for the 16-QAM constellation, these optimum values are $\theta_1^{'} = \arctan(4), \theta_2^{'} = \arctan(0.25)$. The maximum coding gain for 4-QAM is found to be 0.8 and for 16-QAM is 0.2353.

B. Maximum Channel Capacity (MCC) Construction

It can be shown that the eigenvalue distribution of the equivalent channel matrix for the MTD STBC in (6) is not the same as that of the original channel matrix due to the induced space-time correlation, hence this design is not an information lossless STBC [3]. Therefore, as we increase N_r or the constellation size, the MTD construction loses coding gain. It is possible, however, to re-design the code to preserve the mutual information between the transmit and received vectors as summarized in the following proposition.

Proposition 2:
Let $\boldsymbol{P}$ be a 2×2 transformation matrix. Introducing $\boldsymbol{R}^{'} \triangleq \begin{bmatrix} a_1 & b_1 \\ a_2 & b_2 \end{bmatrix} = \boldsymbol{P}\boldsymbol{R}$, where $\boldsymbol{R}$ is defined in (5), our goal is to design $\boldsymbol{P}$ such that the STBC

$$\begin{aligned} \boldsymbol{v} &\triangleq \operatorname{diag}\left(\boldsymbol{R}^{'} \left[\begin{array}{cc} \mathcal{V}_1^{'} & \mathcal{V}_2^{'} \end{array}\right]\right) + \operatorname{diag}\left(\boldsymbol{R}^{'} \left[\begin{array}{cc} \mathcal{V}_1 & \mathcal{V}_2 \end{array}\right] J\right) J \\ &= \begin{bmatrix} s_1^{'} a_1 - s_2^{'*} b_1 & s_3^* b_1 + s_4 a_1 \\ s_3 a_2 - s_4^* b_2 & s_1^{'*} b_2 + s_2^{'} a_2 \end{bmatrix} \end{aligned} \quad (11)$$

is information lossless. This is achieved by the following $\boldsymbol{R}^{'}$

$$\boldsymbol{R}^{'} = \begin{bmatrix} \alpha_1 & \beta_1 \\ \beta_2 & \alpha_2 \end{bmatrix} \quad (12)$$

where $\alpha_1, \beta_1, \alpha_2, \beta_2$ are the MTD design parameters. Comparing the forms of $\boldsymbol{R}^{'}$ and $\boldsymbol{R}$, we can see that the MTD and MCC constructions are related through a simple permutation of the elements on the second row of $\boldsymbol{R}$.

Proof: See Appendix II. ■

IV. Decoding

In this section, we propose a reduced-complexity decoding algorithm which achieves the performance of full ML decoding. Since the MTD and MCC constructions have the same algebraic structure (i.e. linear combination of two Alamouti STBC), the same decoding algorithm can be used for both constructions. To decode the STBC schemes in [3], [4], [5], [6], a size-q^4 exhaustive ML search has to be performed over all 4 information symbols transmitted in each codeword. Therefore, real-time implementation of these schemes is challenging in practical systems, especially for large signal constellations. Any suboptimal receiver such as zero-forcing, minimum mean square error (MMSE) or ordered successive interference cancellation (OSIC), will degrade their performance significantly compared to full ML decoding. Hence, the ultimate goal of these STBC schemes which is to achieve the optimum diversity-multiplexing trade-off would not be accomplished due to this performance loss. While the sphere decoding algorithm is one of the most efficient methods for solving the *integer least square problem* with finite constellations [17], it does not provide polynomial decoding complexity for large problem sizes [18]. Here, the problem size is defined as the number of symbols that are to be jointly decoded. In fact, the expected complexity of sphere decoding which is defined as the sum of the number of lattice points inside the sphere of radius r, grows exponentially with the problem size [18]. This is primarily due to the fact that for low-to-intermediate SNR levels or ill-conditioned channel matrices, the probability of finding a lattice point inside the sphere makes r so large that it captures a substantial fraction of the lattice points. For our code, we perform a conditional ML search to decode $s_2^{'}$ and s_3 and cancel their interference from the received signals followed by simple matched-filtering for information symbols $s_1^{'}$ and s_4. This algorithm achieves the optimum ML performance since the resulting equivalent channel after cancellation of the first two symbols is orthogonal and, therefore, ML decoding is equivalent to simple matched-filtering. Assuming transmission of MCC, by expanding (1) and taking the complex conjugate of y_{r2} for $r = 1, \cdots, N_r$, we can re-write (1) as follows

$$\boldsymbol{\mathcal{Y}} = \sqrt{\frac{\rho}{N_t}} \boldsymbol{\mathcal{H}} \boldsymbol{s}^{'} + \boldsymbol{w}^{'} \quad (13)$$

where $\boldsymbol{\mathcal{Y}} = [y_{11}, y_{12}^*, \cdots, y_{N_r 1}, y_{N_r 2}^*]^T$ and $\boldsymbol{s}^{'} = [s_1^{'}, s_2^{'*}, s_3, s_4^*]^T$ and $\boldsymbol{w}^{'} = [w_1, w_2^*, \cdots, w_{2N_r}^*]^T$. The equivalent channel matrix $\boldsymbol{\mathcal{H}}$ is

$$\boldsymbol{\mathcal{H}} = \begin{bmatrix} h_{11}a_1 & -h_{11}b_1 & h_{12}a_2 & -h_{12}b_2 \\ h_{12}^* b_2 & h_{12}^* a_2 & h_{11}^* b_1 & h_{11}^* a_1 \\ \vdots & \vdots & \vdots & \vdots \\ h_{N_r 1}a_1 & -h_{N_r 1}b_1 & h_{N_r 2}a_2 & -h_{N_r 2}b_2 \\ h_{N_r 2}^* b_2 & h_{N_r 2}^* a_2 & h_{N_r 1}^* b_1 & h_{N_r 1}^* a_1 \end{bmatrix} \quad (14)$$

Canceling $s_2^{'}$ and s_3, the second and the third columns of $\boldsymbol{\mathcal{H}}$ are eliminated. Denoting the resulting equivalent channel matrix (after cancellation) by $\mathbb{H}$, we can write

$$\mathbb{Y} = \mathbb{H} \begin{bmatrix} s_1^{'} \\ s_4^* \end{bmatrix} + \mathbb{W} \quad (15)$$

It can be easily verified that the columns of $\mathbb{H}$ are orthogonal to each other and therefore ML decoding of $s_1^{'}$ and s_4^* is decoupled.

V. Differential Transmission

Channel estimation in a fast time-varying communication environment is computationally expensive and can result in substantial data rate loss due to training overhead. Moreover, considering the increased number of unknown channel coefficients in a MIMO system, it is sometimes desirable to eliminate channel estimation at the receiver at the cost of some performance loss. In this section, we investigate differential transmission for our proposed code and derive the exact ML differential decoding metric. Furthermore, we derive a suboptimal reduced-complexity differential decoding metric and compare its performance with the differential ML decoder for both the MTD and Golden codes. Interestingly, the suboptimal and the ML differential decoding metrics for our code achieve almost the same performance while there is a bigger performance loss for the Golden code. [3]

A. Differential Encoder

Assuming differential transmission of M MTD [4]codewords and denoting the kth transmitted codeword by $\boldsymbol{X}(k)$ for $0 \leq k \leq M-1$. The differential scheme is initialized by transmitting $\boldsymbol{X}(0) = \boldsymbol{I_2}$, where $\boldsymbol{I_2}$ is the 2×2 identity matrix, and proceeds as follows

$$\boldsymbol{B}(k) = \boldsymbol{X}(k-1)\boldsymbol{u}(k); \qquad \boldsymbol{X}(k) = \frac{\boldsymbol{B}(k)}{\sqrt{e(k)}} \tag{16}$$

The total transmitted energy from all antennas is constrained to be a constant independent of N_t; i.e.

$$\mathsf{E}\left[\sum_{r=1}^{N_r}\sum_{m=1}^{N_t}|x_{m,r}(k)|^2\right] = t \tag{17}$$

where $\boldsymbol{X}(k-1)$ and $\boldsymbol{X}(k)$ are the transmitted codewords at times $(k-1)$ and k, respectively, and $e(k)$ is the energy normalizer i.e. $e(k) = \frac{tr\{\boldsymbol{B}(k)\boldsymbol{B}^H(k)\}}{t}$. Hence, the energy constraint in (17) is satisfied since

$$\begin{aligned} t &= \mathsf{E}\left[\sum_{r=1}^{N_r}\sum_{m=1}^{N_t}|x_{m,r}(k)|^2\right] = \mathsf{E}\left[tr\left\{\boldsymbol{X}(k)\boldsymbol{X}^H(k)\right\}\right] \\ &= \mathsf{E}\left[tr\left\{\frac{\boldsymbol{B}(k)\boldsymbol{B}^H(k)}{\frac{tr\{\boldsymbol{B}(k)\boldsymbol{B}^H(k)\}}{t}}\right\}\right] \\ &= \mathsf{E}\left[\frac{t}{tr\{\boldsymbol{B}(k)\boldsymbol{B}^H(k)\}}tr\{\boldsymbol{B}(k)\boldsymbol{B}^H(k)\}\right] \end{aligned} \tag{18}$$

Keeping the average transmitted energy constant is critical here in the differential encoder since the MTD code is not orthogonal and successive multiplication of the codewords may cause its energy to blow up or diminish. The corresponding received signal blocks over codeword transmissions k and $k-1$ are

$$\begin{aligned} [\boldsymbol{Y}(k-1) \quad \boldsymbol{Y}(k)] = [&\boldsymbol{H}(k-1)\boldsymbol{X}(k-1) \quad \boldsymbol{H}(k)\boldsymbol{X}(k)] \\ &+ [\boldsymbol{W}(k-1) \quad \boldsymbol{W}(k)] \end{aligned} \tag{19}$$

Substituting (16) into (19) and applying the quasi-static channel assumption $\boldsymbol{H}(k) = \boldsymbol{H}(k-1)$, we can write

$$\boldsymbol{Y}(k) = \frac{\boldsymbol{Y}(k-1)\boldsymbol{u}(k)}{\sqrt{e(k)}} + \tilde{\boldsymbol{W}}(k) \tag{20}$$

where the equivalent noise matrix seen by the differential decoder is given by

$$\tilde{\boldsymbol{W}}(k) = \boldsymbol{W}(k) - \frac{\boldsymbol{W}(k-1)\boldsymbol{u}(k)}{\sqrt{e(k)}} \tag{21}$$

B. Differential Decoding

Due to the non-orthogonality of the MTD code, its ML differential decoding can not be performed using simple linear processing as in OSTBC [21] and an exhaustive search is needed in general whose complexity increases exponentially with the constellation size and the number of transmit antennas. Starting from (19), we can derive the ML decoding rule for our non-orthogonal differential MTD as follows. Define

$$\begin{aligned} \boldsymbol{Y_E} &\triangleq [\boldsymbol{Y}(k) \quad \boldsymbol{Y}(k-1)] \\ &= \boldsymbol{H}(k)\,[\boldsymbol{X}(k) \quad \boldsymbol{X}(k-1)] + [\boldsymbol{W}(k) \quad \boldsymbol{W}(k-1)] \\ &= \boldsymbol{H}(k)\left[\boldsymbol{X}(k-1)\boldsymbol{u}^{'}(k) \quad \boldsymbol{X}(k-1)\right] \\ &+ [\boldsymbol{W}(k) \quad \boldsymbol{W}(k-1)] \\ &= \boldsymbol{H}(k)\boldsymbol{X}(k-1)\left[\boldsymbol{u}^{'}(k) \quad \boldsymbol{I_2}\right] + [\boldsymbol{W}(k) \quad \boldsymbol{W}(k-1)] \\ &\triangleq \boldsymbol{H_E}\boldsymbol{G} + \boldsymbol{W_E} \end{aligned} \tag{22}$$

where $\boldsymbol{H_E} \triangleq \boldsymbol{H}(k)\boldsymbol{X}(k-1)$ and $\boldsymbol{u}^{'}(k) = \frac{\boldsymbol{u}(k)}{\sqrt{e(k)}}$. Since $\boldsymbol{W_E} = [\boldsymbol{W}(k) \quad \boldsymbol{W}(k-1)]$ is AWGN and *independent* of $\boldsymbol{G}$, we can write the exact ML decoding metric as follows

$$J_{ML} = \arg\min \|\boldsymbol{Y_E} - \boldsymbol{H_E}\boldsymbol{G}\|^2 \tag{23}$$

We can eliminate the dependence of J_{ML} on $\boldsymbol{H_E}$ by differentiating J_{ML} with respect to $\boldsymbol{H_E}$ to find the choice of $\boldsymbol{H_E}$ which minimizes J_{ML}. Using the the derivative rules of a quadratic function consists of a matrix and vectors we get

$$\boldsymbol{H_E} = (\boldsymbol{Y}(k)\boldsymbol{u}^{'H}(k) + \boldsymbol{Y}(k-1))(\boldsymbol{I_2} + \boldsymbol{u}^{'}(k)\boldsymbol{u}^{'H}(k))^{-1} \tag{24}$$

Substituting back for $\boldsymbol{H_E}$ from (24) into (23), we get

$$\begin{aligned} J_{ML} = \arg\min\{&\|\boldsymbol{Y}(k) - (\boldsymbol{Y}(k)\boldsymbol{u}^{'H}(k) + \boldsymbol{Y}(k-1)) \\ &(\boldsymbol{I_2} + \boldsymbol{u}^{'}(k)\boldsymbol{u}^{'H}(k))^{-1}\boldsymbol{u}^{'}(k)\|^2 \\ &+ \|\boldsymbol{Y}(k-1) - (\boldsymbol{Y}(k)\boldsymbol{u}^{'H}(k) + \boldsymbol{Y}(k-1)) \\ &(\boldsymbol{I_2} + \boldsymbol{u}^{'}(k)\boldsymbol{u}^{'H}(k))^{-1}\|^2\} \end{aligned}$$

[3]We emphasize that conventional differential OSTBC schemes [20] [21] do not apply to the non-orthogonal STBC considered in this paper.

[4]The same approach can be followed for the MCC code as well.

This metric is very complex to implement. Using (20), the following *approximate* ML decoder can be derived by minimizing the following suboptimal[5] metric

$$J_{ML}^{\text{approx}} = \arg\min \left\| \boldsymbol{Y}(k) - \frac{\boldsymbol{Y}(k-1)\boldsymbol{u}(k)}{\sqrt{e(k)}} \right\|^2 \quad (25)$$

The performances of the metrics J_{ML}^{approx} and J_{ML} will be compared in Section VIII for both the MTD construction and the Golden code. Note that J_{ML} collapses to J_{ML}^{approx} for orthogonal STBC[6]. Even more important are the two observations that the differential MTD code outperforms the differential Golden code and that the performance gap between differential and coherent decoding is less for the MTD code than for the Golden code.

VI. Multiple-Access Channels

Without loss of generality, we consider two perfectly-synchronous users each using the MCC STBC[7] of Section III-B trying to access the base station using spatial division multiple access (SDMA) with signal-to-interference-noise ratio (SINR) of 0 dB; i.e. both users are operating at the same power level which is a very challenging scenario. The base station processes the received signals from the two users during $t = 2$ time slots. For the linear decorrelation of the two users to be possible at the base station, we need $N_r \geq 4$ receive antennas since there are 8 information symbols from the two users to be jointly decoded. The uplink input-output model can be written in terms of the equivalent channel matrix including the interference from the other user by generalizing (13) as follows

$$\begin{bmatrix} \boldsymbol{\mathcal{Y}_1} \\ \boldsymbol{\mathcal{Y}_2} \end{bmatrix} = \sqrt{\frac{\rho}{N_t}} \begin{bmatrix} \boldsymbol{\mathcal{H}_1} & \boldsymbol{\mathcal{Q}_1} \\ \boldsymbol{\mathcal{Q}_2} & \boldsymbol{\mathcal{H}_2} \end{bmatrix} \begin{bmatrix} \boldsymbol{s_1'} \\ \boldsymbol{s_2'} \end{bmatrix} + \begin{bmatrix} \boldsymbol{w_1'} \\ \boldsymbol{w_2'} \end{bmatrix} \quad (26)$$

where $\boldsymbol{\mathcal{Y}_i}$ for $i = 1, 2$ are the received signal vectors of length $2N_r$ each, $\boldsymbol{\mathcal{H}_i}$ for $i = 1, 2$ are the $2N_r \times 4$ channel matrices between each user and the base station and $\boldsymbol{\mathcal{Q}_j}$ for $j = 1, 2$ are the $2N_r \times 4$ channel matrices corresponding to interference from the other user. Multiplying by the linear decorrelator matrix $\boldsymbol{\mathcal{D}}$, the base station receiver cancels the interference from the other user at the expense of possible noise enhancement [8]

$$\begin{bmatrix} \tilde{\boldsymbol{\mathcal{Y}}}_1 \\ \tilde{\boldsymbol{\mathcal{Y}}}_2 \end{bmatrix} = \sqrt{\frac{\rho}{N_t}} \begin{bmatrix} \tilde{\boldsymbol{\mathcal{H}}} & \boldsymbol{0} \\ \boldsymbol{0} & \tilde{\boldsymbol{\mathcal{Q}}} \end{bmatrix} \begin{bmatrix} \boldsymbol{s_1'} \\ \boldsymbol{s_2'} \end{bmatrix} + \boldsymbol{\mathcal{D}} \begin{bmatrix} \boldsymbol{w_1'} \\ \boldsymbol{w_2'} \end{bmatrix} \quad (27)$$

Define the following partitioning of the decorrelator matrix $\boldsymbol{\mathcal{D}} \triangleq \begin{bmatrix} \boldsymbol{\mathcal{D}_1} & \boldsymbol{\mathcal{D}_2} \\ \boldsymbol{\mathcal{D}_3} & \boldsymbol{\mathcal{D}_4} \end{bmatrix}$. Then to decouple the two users as in (27), we must have

$$\begin{aligned} \boldsymbol{\mathcal{D}_2} &= -\boldsymbol{\mathcal{D}_1}\boldsymbol{\mathcal{Q}_1}(\boldsymbol{\mathcal{H}_2}^H\boldsymbol{\mathcal{H}_2})^{-1}\boldsymbol{\mathcal{H}_2}^H \\ \boldsymbol{\mathcal{D}_3} &= -\boldsymbol{\mathcal{D}_4}\boldsymbol{\mathcal{Q}_2}(\boldsymbol{\mathcal{H}_1}^H\boldsymbol{\mathcal{H}_1})^{-1}\boldsymbol{\mathcal{H}_1}^H \end{aligned} \quad (28)$$

The autocorrelation matrix of the filtered noise at the output of the decorrelator is given by $\boldsymbol{R_{w'w'}} = \sigma^2\boldsymbol{\mathcal{D}}\boldsymbol{\mathcal{D}}^H$. Therefore, $\boldsymbol{\mathcal{D}_1}$ and $\boldsymbol{\mathcal{D}_4}$ can be designed to make the filtered noise variance equal to the original white noise variance as follows (the details are straightforward and omitted here because of space limitations.)

$$\begin{aligned} \boldsymbol{\mathcal{D}_1} &= \left[\boldsymbol{I} + \boldsymbol{\mathcal{Q}_1}(\boldsymbol{\mathcal{H}_2}^H\boldsymbol{\mathcal{H}_2})^{-1}\boldsymbol{\mathcal{Q}_1}^H\right]^{-\frac{1}{2}} \\ \boldsymbol{\mathcal{D}_4} &= \left[\boldsymbol{I} + \boldsymbol{\mathcal{Q}_2}(\boldsymbol{\mathcal{H}_1}^H\boldsymbol{\mathcal{H}_1})^{-1}\boldsymbol{\mathcal{Q}_2}^H\right]^{-\frac{1}{2}} \end{aligned} \quad (29)$$

The second stage of decoding consists of performing ML detection on the decoupled information vectors $\boldsymbol{s_1'}$ and $\boldsymbol{s_2'}$ from each user separately. This can be done using the reduced-complexity HMLIC algorithm proposed in Section IV for the single-user case.

Proposition 3:
The equivalent channel matrices $\tilde{\boldsymbol{\mathcal{H}}}$ and $\tilde{\boldsymbol{\mathcal{Q}}}$ at the output of the decorrelator in (27) have two pairs of orthogonal columns and, therefore, HMLIC detection is ML-optimal for both decorrelated users analogous to the single-user case.
Proof: See Appendix III. ■

VII. Frequency-Selective Channels

In this section, we show how to integrate our MTD STBC code with equalization for transmission over frequency-selective channels [9]. This is achieved by implementing it at a block level to combat the frequency selectivity of the channel and performing MMSE-based single-carrier frequency-domain equalization (SC-FDE) [19] to decode the transmitted information blocks. The MMSE SC-FDE has two major advantages over orthogonal frequency division multiplexing (OFDM). First, it has a lower peak-to-average ratio (PAR) which makes it suitable especially for our proposed MTD and MCC codes since they transmit linear combinations of the information symbols which can result in high PAR. Second, the SC-FDE has lower sensitivity to carrier frequency offset than OFDM. When the channel maximum delay spread exceeds the symbol period, transmissions are impaired by inter-symbol interference (ISI). Assume that the maximum delay spread between the $N_r \times N_t$ channel paths is L and define $h_{rm}(l)$ as the lth channel tap between the mth transmit antenna and the rth receive antenna where $r \in [1, N_r], m \in [1, N_t], l \in [0, L]$. We generate 4 information blocks each of length N and combine them in the time domain so that after DFT processing at the receiver, we get the MTD code structure in the frequency domain. To make the channel matrices circulant, a cyclic prefix of length L is appended at the end of each information block in the time domain. Denoting the nth symbol of the kth transmitted block over the mth transmit antenna by $u_m^k(n)$ we can write

$$\begin{aligned} u_1^k(n) &= \alpha_1 s_1^k(n) - \beta_1 s_2^{*k}([N-n]_N) \\ u_2^k(n) &= \alpha_2 s_3^k(n) - \beta_2 s_4^{*k}([N-n]_N) \end{aligned} \quad (30)$$

where $[\cdot]_N$ is the modulo-N operation. Equation (30) can be represented in vector notation as follows

$$\boldsymbol{u_1^k} = \alpha_1\boldsymbol{s_1^k} - \beta_1\overline{\boldsymbol{s_2^k}}; \qquad \boldsymbol{u_2^k} = \alpha_2\boldsymbol{s_3^k} - \beta_2\overline{\boldsymbol{s_4^k}} \quad (31)$$

[5]This metric is suboptimal since the equivalent noise term $\tilde{\boldsymbol{W}}(k)$ in (20) is not white and is dependent on $\boldsymbol{u}'(k)$.

[6]This can be easily verified by substituting $\boldsymbol{u}'(k)\boldsymbol{u}'^H(k) = \boldsymbol{I_2}$ in the expression for J_{ML}.

[7]The same approach can be used for MTD code as well.

[8]For simplicity, a zero-forcing design for $\boldsymbol{\mathcal{D}}$ is considered in this paper, however, the MMSE design derivation is straightforward.

[9]The same approach can be used for the MCC code as well.

where $\overline{[\cdot]}$ stands for the complex-conjugate operation over a vector of length N. The received block from the rth receive antenna during the kth block transmission in the time domain is given by

$$\begin{aligned} \boldsymbol{y_r^k} &= \boldsymbol{H_{c_{1r}}}\left(\alpha_1 \boldsymbol{s_1^k} - \beta_1 \overline{\boldsymbol{s_2^k}}\right) \\ &\quad + \boldsymbol{H_{c_{2r}}}\left(\alpha_2 \boldsymbol{s_3^k} - \beta_2 \overline{\boldsymbol{s_4^k}}\right) + \boldsymbol{w_r^k} \end{aligned} \tag{32}$$

where $\boldsymbol{H_{c_{mr}}}$ is the circulant channel matrix from the mth transmit antenna to the rth receive antenna. Assuming quasi-static channels, the channel taps remain constant over two consecutive block transmissions. Performing the same block processing for the $(k+1)$th block transmission, the $(k+1)$th received block in the time domain is given by

$$\begin{aligned} \boldsymbol{y_r^{k+1}} &= \boldsymbol{H_{c_{1r}}}\left(\beta_1 \overline{\boldsymbol{s_3^{k+1}}} + \alpha_1 \boldsymbol{s_4^{k+1}}\right) \\ &\quad + \boldsymbol{H_{c_{2r}}}\left(\alpha_2 \boldsymbol{s_2^{k+1}} + \beta_2 \overline{\boldsymbol{s_1^{k+1}}}\right) + \boldsymbol{w_r^{k+1}} \end{aligned} \tag{33}$$

Since all channel matrices are circulant, they can be diagonalized using the DFT orthonormal matrix $\boldsymbol{F}$ whose (p,q) element is given by $\boldsymbol{F}(p,q) = \frac{1}{\sqrt{N}}\exp(-j\frac{2\pi pq}{N})$ for $0 \leq p,q \leq N-1$. At the receiver, the time domain blocks are transformed to the frequency domain by first removing the cyclic prefix and then multiplying by $\boldsymbol{F}$ as follows

$$\begin{aligned} \boldsymbol{Y_r^k} &\triangleq \boldsymbol{F}\boldsymbol{y_r^k} \\ &= \boldsymbol{F}\boldsymbol{F}^H \boldsymbol{D_{r1}}\boldsymbol{F}\left(\alpha_1 \boldsymbol{s_1^k} - \beta_1 \overline{\boldsymbol{s_2^k}}\right) \\ &\quad + \boldsymbol{F}\boldsymbol{F}^H \boldsymbol{D_{r2}}\boldsymbol{F}\left(\alpha_2 \boldsymbol{s_3^k} - \beta_2 \overline{\boldsymbol{s_4^k}}\right) + \boldsymbol{F}\boldsymbol{w_r^k} \\ &= \boldsymbol{D_{r1}}\left(\alpha_1 \boldsymbol{S_1^k} - \beta_1 \boldsymbol{S_2^{*k}}\right) + \boldsymbol{D_{r2}}\left(\alpha_2 \boldsymbol{S_3^k} - \beta_2 \boldsymbol{S_4^{*k}}\right) + \boldsymbol{W_r^k} \end{aligned} \tag{34}$$

where $\boldsymbol{S_i^k} = \boldsymbol{F}\boldsymbol{s_i^k}$, $i = 1, \cdots, 4$ are the transmitted blocks in the frequency domain and $\boldsymbol{D_{rm}}$ is $N \times N$ diagonal matrix with (n,n) element given by

$$\boldsymbol{D_{rm}}(n,n) = \frac{1}{\sqrt{N}} \sum_{l=0}^{L} h_{r,m}(l) e^{-j\frac{2\pi nl}{N}} \qquad m = 1,2 \quad r = 1, \cdots, N_r \tag{35}$$

Following the same procedure, one can derive the received block during the $(k+1)$th block transmission to be

$$\begin{aligned} \boldsymbol{Y_r^{k+1}} &= \boldsymbol{D_{r1}}\left(\beta_1 \boldsymbol{S_3^{*k+1}} + \alpha_1 \boldsymbol{S_4^{k+1}}\right) \\ &\quad + \boldsymbol{D_{r2}}\left(\alpha_2 \boldsymbol{S_2^{k+1}} + \beta_2 \boldsymbol{S_1^{*k+1}}\right) + \boldsymbol{W_r^{k+1}} \end{aligned} \tag{36}$$

Taking the element-wise complex conjugation of $\boldsymbol{Y_r^{k+1}}$ and collecting all the received blocks from the N_r receive antennas, we get the system of equations in the frequency domain shown in (37) at the top of the next page. Note that (37) can be viewed as a frequency-domain vectorized-form of the time-domain relations in (13). Also note that performing HMLIC to decode (37) is not possible because equalization is done in the frequency-domain where the lattice structure (due to the signal constellation) has been destroyed by the application of the DFT matrix. Instead, we consider the MMSE estimate of the nth element of each of 4 received blocks in the frequency-domain which is given by

$$\hat{\boldsymbol{S}}^{\boldsymbol{k}}(n) = \left(\boldsymbol{D}^H(n,n)\boldsymbol{D}(n,n) + \frac{N_t}{\rho}\boldsymbol{I}_4\right)^{-1} \boldsymbol{D}^H(n,n)\boldsymbol{Y^k}(n) \tag{38}$$

where $\hat{\boldsymbol{S}}^{\boldsymbol{k}}(n) = [\boldsymbol{S_1^k}(n) \;\; \boldsymbol{S_2^{*k}}(n) \;\; \boldsymbol{S_3^k}(n) \;\; \boldsymbol{S_4^{*k}}(n)]^T$ is a 4×1 vector of the MMSE estimates of the nth symbols from each of the 4 information blocks. Similarly, $\boldsymbol{D}(n,n)$ is a $2N_r \times 4$ matrix constructed from the channel gains $\boldsymbol{D_{rm}}(n,n)$ at the nth frequency-domain bin defined in (35). In addition, $\boldsymbol{Y^k}(n) = [\boldsymbol{Y_1^k}(n) \;\; \boldsymbol{Y_1^{*k+1}}(n) \cdots \boldsymbol{Y_{N_r}^k}(n) \;\; \boldsymbol{Y_{N_r}^{*k+1}}(n)]^t$ is the vector of the nth elements from each of the 4 received blocks. Therefore, MMSE-based SC-FDE is performed over the nth elements of the 4 information blocks in the frequency domain. Stacking all symbol estimates in vectors, they can be transformed back to the time domain followed by a slicer to decode the information blocks.

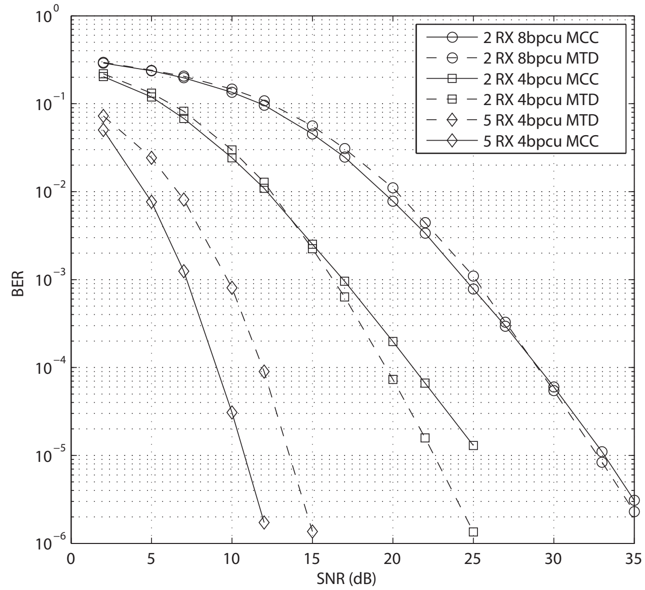

Fig. 1. Comparison of MTD and MCC constructions with different number of receive antennas and different spectral efficiencies. 4 and 8 bpcu are equivalent to using 4-QAM and 16-QAM, respectively.

VIII. Simulation Results

In this section, we present simulation results for our new code (both MTD and MCC constructions) and compare it with the Golden and $B_{2,\phi}$ codes in [6] and [3], respectively. We also compare the performance of our code with the recently proposed STBCs in [8], [9], [10].

A natural question to ask at this point is when to use MTD or MCC constructions? To answer this question, the BER performances of the MTD and MCC constructions are compared under different transmission scenarios in Fig.1. It can be seen from this figure that when the number of receive antennas and the spectral efficiency are small, the MTD construction achieves better performance since achieving full diversity is more critical than full capacity under these scenarios. However, as we increase the number of receive antennas, the capacity of the underlying MIMO channel will increase and hence preserving the mutual information between the transmit and the received signal vectors becomes more crucial. The

$$\begin{bmatrix} Y_1^k \\ Y_1^{*k+1} \\ \vdots \\ Y_{N_r}^k \\ Y_{N_r}^{*k+1} \end{bmatrix} = \begin{bmatrix} D_{11}\alpha_1 & -D_{11}\beta_1 & D_{12}\alpha_1 & -D_{12}\beta_1 \\ D_{12}{}^*\alpha_2 & D_{12}{}^*\beta_2 & D_{11}{}^*\alpha_2 & D_{11}{}^*\beta_2 \\ \vdots & \vdots & \vdots & \vdots \\ D_{N_r1}\alpha_1 & -D_{N_r1}\beta_1 & D_{N_r2}\alpha_1 & -D_{N_r2}\beta_1 \\ D_{N_r2}{}^*\alpha_2 & D_{N_r2}{}^*\beta_2 & D_{N_r1}{}^*\alpha_2 & D_{N_r1}{}^*\beta_2 \end{bmatrix} \begin{bmatrix} S_1^k \\ S_2^{*k} \\ S_3^k \\ S_4^{*k} \end{bmatrix} + \begin{bmatrix} W_1^k \\ W_1^{*k+1} \\ \vdots \\ W_{N_r}^k \\ W_{N_r}^{*k+1} \end{bmatrix} \quad (37)$$

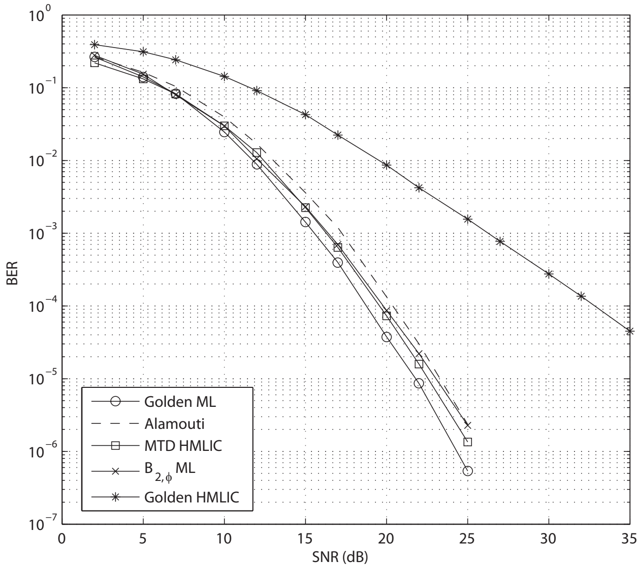

Fig. 2. Bit error rate performance of the MTD code with $N_r = 2$ and the spectral efficiency of 4 bits pcu.

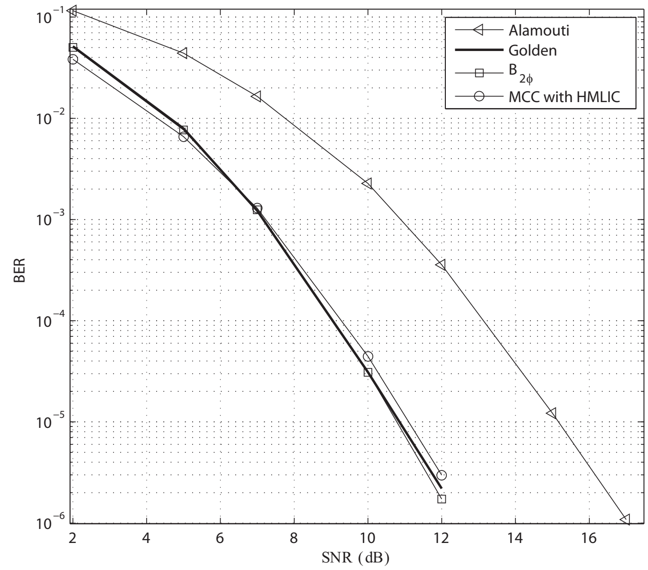

Fig. 3. Bit error rate performance of the MCC code with $N_r = 5$ and the spectral efficiency of 4 bits pcu.

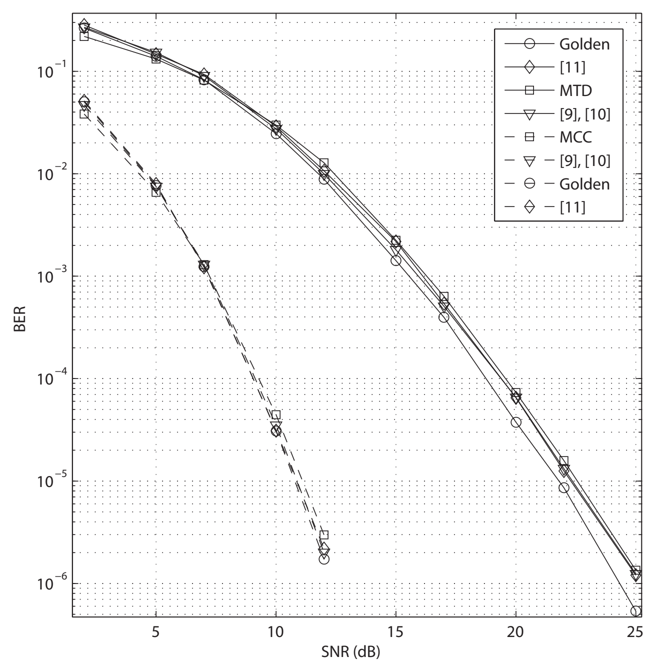

Fig. 4. Comparison between MTD and MCC with the codes in [8], [9] and [10] and . The dashed curves are for comparison of MCC with others using 5 receive antennas. The solid curves are for comparison of MTD with others using 2 receive antennas. Spectral efficiency is 4 bits pcu.

same trend also holds as we increase the signal constellation size and the MCC construction becomes preferable in this case as well.

Next, in Fig.2 the BER comparison is extended to $N_r = 2$ and a transmission rate of 4 bits pcu. It is clear that the MTD code outperforms the Alamouti and $B_{2,\phi}$ codes over all SNR values considered and has less than 1dB performance loss (at high SNR) compared to the Golden code [6] since the MTD code does not achieve full channel capacity [17]. However, the reduced ML decoding complexity of the MTD code still makes it attractive for practical implementation compared to the Golden code. It can be seen from Fig.2, that if we use the same low-complexity HMLIC algorithm to decode the Golden code, the BER degrades significantly since the Golden code's equivalent channel (after interference cancellation) is not orthogonal and hence matched-filtering is highly suboptimal.

Next, we examine in Fig.3 the BER of our MCC code in comparison with the Alamouti, Golden and $B_{2,\phi}$ codes for $N_r = 5$ at a spectral efficiency of 4 bits pcu where we observe about 4dB loss for the Alamouti code compared to the other 3 codes. This is expected because the Alamouti code is not information lossless for $N_r > 1$. Note that although our MCC code suffers from a diversity loss compared to the Golden and $B_{2\phi}$ codes, their performance is nearly identical to our code for the considered SNR range which is typical for many wireless channels.

Fig.4 shows a performance comparison of MTD with those of [8], [10][10], and [9] with $N_r = 2$ and spectral efficiency of 4 bits pcu. In the same figure, MCC is compared with the schemes in [8], [9] and [10] in the presence of $N_r = 5$ receive antennas and spectral efficiency of 4 bits pcu. As it can be seen from this figure, if the right construction i.e. MTD or MCC is used in the right transmission environment, then the BER

[10]As pointed out in [13], the codes in [8] and [9] are identical.

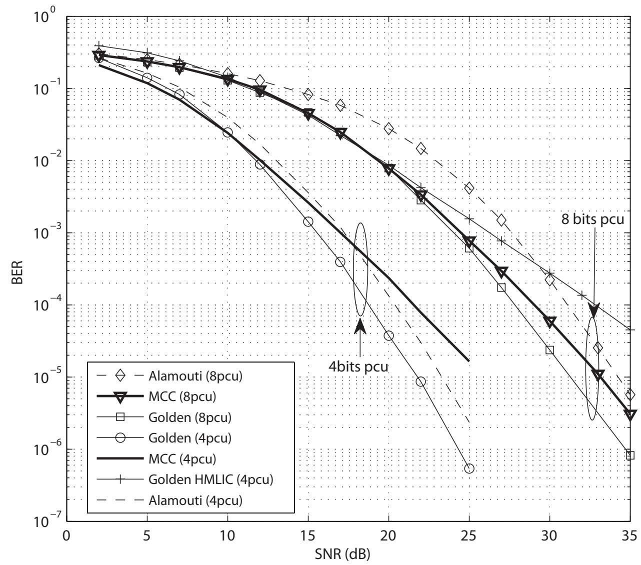

Fig. 5. Bit error rate performance of the MCC code with $N_r = 2$ and spectral efficiencies of 4 bits pcu and 8 bits pcu.

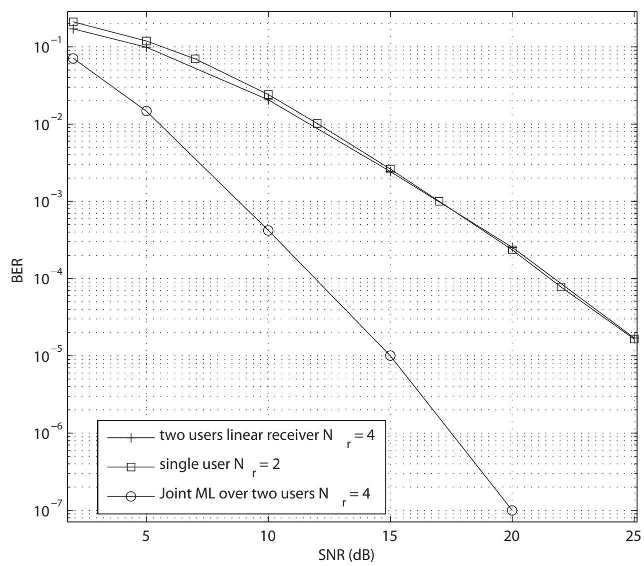

Fig. 7. BER performance comparison between the single-user and two-user scenarios with the MCC code assuming QPSK constellation.

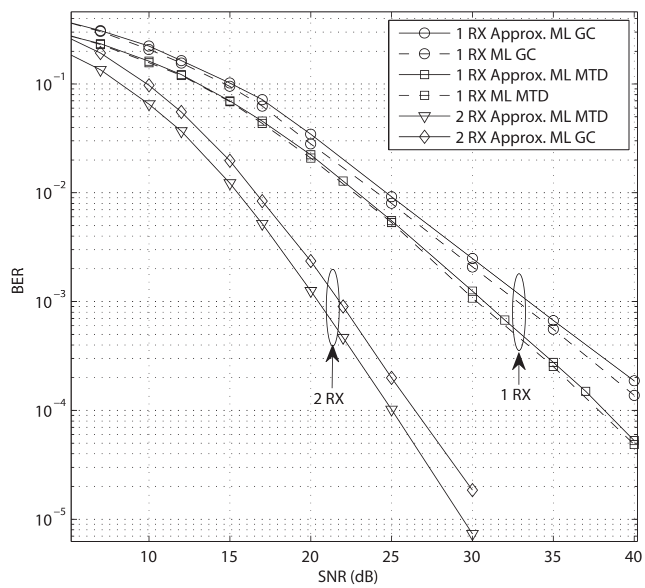

Fig. 6. BER comparison between J_{ML} and J_{ML}^{approx} assuming differential transmission for the MTD and Golden codes with QPSK constellation and 1 and 2 receive antennas.

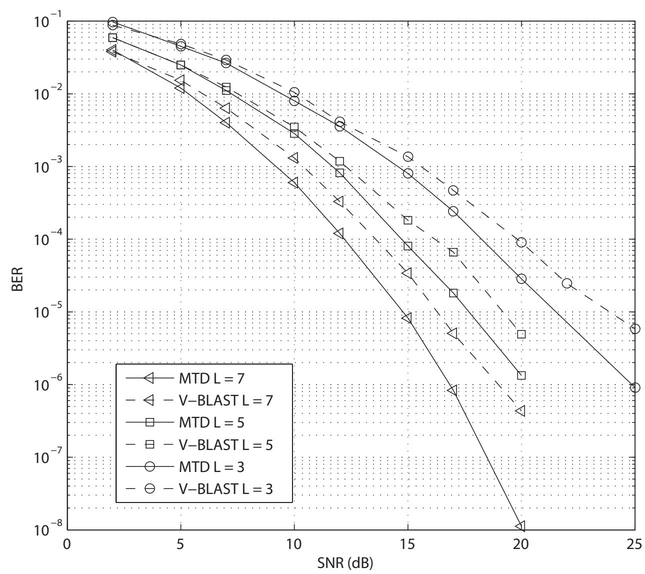

Fig. 8. BER performance of the MMSE SC-FDE receiver with the MTD code compared with V-BLAST for different channel delay spread $L = 3, 5, 7$ at the rate of 4 bits pcu and $N_r = 2$.

performances of these schemes are almost the same.

It is interesting to note here that although the coding gain of our MTD code construction is inferior to the coding gains of the codes in [9], [10], [4] (as Table I shows), the error rate performance is almost identical for all of these codes. This observation corroborates the observation made in [16] that the error rate in STBC systems is not only determined by the coding and diversity gains but also by the number of nearest neighbors.

Fig.5 depicts the BER performance of our MCC code for $N_r = 2$ receive antennas for two different transmission rates of 4 bits pcu and 8 bits pcu. It is clear that the diversity loss compared to the Golden code [6] is noticeable only for the lower-rate scenario of 4 bits pcu and SNR greater than 12 dB. For the higher-rate scenario of 8 bits pcu, the performance of our code is almost identical to the Golden code for SNR less than 25 dB and it outperforms the Alamouti code for all SNR values under consideration.

Next, we compare in Fig.6 the BER performance of the J_{ML} and J_{ML}^{approx} differential decoder metrics for the MTD and Golden codes with $N_r = 1, 2$ and 4-QAM constellation. Thanks to the special algebraic structure of the MTD code, the performance gap between the two metrics is not as high as that of the Golden code for $N_r = 1$. Furthermore, it is clear that the differential MTD code outperforms the differential Golden code by about 2.2dB at high SNR for $N_r = 1$. Moreover, comparing the performances of the MTD and Golden code differential schemes with their corresponding coherent ones shown in Fig.6 at BER of 10^{-3}, there is a loss of about 4.2dB for the MTD code and 5.8dB for the Golden code. These losses exceed the theoretical minimum of 3dB which is achieved by orthogonal STBC. For $N_r = 2$, there is still about 1.8dB performance improvement with respect to the differential Golden code despite the fact that the Golden code performs better than the MTD code with coherent detection for $N_r = 2$.

Fig.7 compares the BER of the MCC code in the single-user case with $N_r = 2$ and HMLIC detection with the two-user case assuming $N_r = 4$ and SINR = 0 dB using two different detection algorithms. The first algorithm is the reduced-complexity two-stage receiver consisting of a decorrelator followed by HMLIC and the second algorithm is the joint size-q^8 ML search over all 8 information symbols of both users. The decorrelator stage uses the two extra receive antennas to cancel the two information streams of the other user and hence achieve the single-user performance. On the other hand, the full joint ML receiver uses the two additional receive antennas to achieve higher spatial diversity and better performance than the single-user case at the expense of a much higher decoding complexity.

Finally, the BER performance of the MTD code is investigated for the frequency-selective channel scenario with $L = 3, 5, 7$ and a block size of $N = 64$. As it can be seen from Fig.8, the MMSE-based SC-FDE is clearly capable of capturing multi-path diversity and outperforms V-BLAST at a spectral efficiency of 4 bits pcu and $N_r = 2$.

IX. Conclusion

We designed a closed-form rate-2 space-time block code for two transmit antennas through a judicious application of rotation and linear combination operations on two parallel Alamouti codes. We presented two different constructions of the proposed code design, related through a simple transformation, where one construction maximizes the diversity gain while the other one guarantees the information lossless property. Both constructions were further optimized analytically to maximize coding gain and their special algebraic structure was exploited to design a low-complexity ML decoding algorithm. Through extensive simulation results, we demonstrated the advantage of our proposed code in striking a practical performance-complexity tradeoff comparable to the most competitive existing schemes. Furthermore, we derived the optimum non-coherent (differential) ML decoding metric for our code and approximated it by a near optimum metric at much lower decoding complexity. Finally, we showed how to apply our proposed code in multiple-access and frequency-selective channels by carefully integrating its decoder with interference cancellation and equalization algorithms, respectively.

Appendix A
Proof of Proposition 1

Equations (7) and (8) can be can be combined as follows

$$\begin{aligned}\Psi_\theta &= \max_{\theta}\min_{\boldsymbol{s}\neq\mathbf{0}} \|\det[\boldsymbol{u}(\boldsymbol{s}_1)-\boldsymbol{u}(\boldsymbol{s}_2)]\| \\ &= \min_{\boldsymbol{s}\neq\mathbf{0}}\max_{\theta} \|(|s_1^d|^2+|s_4^d|^2)\alpha_1\beta_2-(|s_2^d|^2+|s_3^d|^2)\beta_1\alpha_2 \\ &\quad+\alpha_1\alpha_2(s_1^d s_2^d - s_3^d s_4^d)-\beta_1\beta_2\left[(s_1^d)^*(s_2^d)^*-(s_3^d)^*(s_4^d)^*\right]\|\end{aligned} \tag{39}$$

where $s_1^d = s_1^{'} - \bar{s}_1^{'}, s_2^d = s_2^{'} - \bar{s}_2^{'}, s_3^d = s_3 - \bar{s}_3, s_4^d = s_4 - \bar{s}_4$ are the difference of the information symbols in the two distinct codewords. Substituting (9) into (39) and introducing the variable $\theta = \theta_1$, we can simplify the coding gain expression as follows

$$\begin{aligned}\Psi_\theta &= \min_{\boldsymbol{s}\neq\mathbf{0}}\max_{\theta} \|\det[\boldsymbol{u}(\boldsymbol{s}_1)-\boldsymbol{u}(\boldsymbol{s}_2)]\| \\ &= \min_{\boldsymbol{s}\neq\mathbf{0}}\max_{\theta} \left\|A\sin^2(\theta)-B\cos^2(\theta)+jC\sin(2\theta)\right\|\end{aligned} \tag{40}$$

where

$$\begin{aligned}&A = |s_1^d|^2+|s_4^d|^2; \qquad B = |s_2^d|^2+|s_3^d|^2 \\ &C = \Im\{s_1^d s_2^d\} - \Im\left\{s_3^d s_4^d\right\}\end{aligned} \tag{41}$$

where $\Im\{\cdot\}$ is the imaginary part operation. Given any feasible values of the constellation-dependent parameters A, B, C, the maximization over θ can be performed by differentiating (40) with respect to θ and setting the result to zero which produces the constellation-independent solution of $\theta = \frac{k\pi}{2}$, and a constellation-dependent solution (which maximizes the coding gain) given by

$$\theta^{\text{opt}} = \arctan\sqrt{\frac{2B^2-4\left(C^2-\frac{1}{2}AB\right)}{2A^2-4\left(C^2-\frac{1}{2}AB\right)}} \tag{42}$$

substituting back the optimum rotation angle θ^{opt} into the expression in (40) we get

$$\Psi_\theta = \min_{\boldsymbol{s}\neq\mathbf{0}} \left\|A\sin^2(\theta^{\text{opt}})-B\cos^2(\theta^{\text{opt}})+jC\sin(2\theta^{\text{opt}})\right\| \tag{43}$$

which gives an expression for the coding gain as a function of the constellation points. Minimization of (43) over $\boldsymbol{s}\neq 0$ for the 4-QAM constellation gives constellation points which when substituted back in (42) result in $\theta^{\text{opt}} = \arctan(0.5)$ as the solution of the optimum rotation angle as we claimed in (10).

Appendix B
Proof of Proposition 2

Considering $\boldsymbol{y} = \sqrt{\frac{\rho}{N_t}}\boldsymbol{H}\boldsymbol{v}+\boldsymbol{w}$, the conditional mutual information between $\boldsymbol{y}$ and $\boldsymbol{v}$ for a given channel realization can be written as

$$\mathcal{I}(\boldsymbol{y},\boldsymbol{v}|\boldsymbol{H}) \triangleq \log_2\det\left(\boldsymbol{I}_{N_r}+\frac{1}{\sigma^2}\boldsymbol{H}R_{\boldsymbol{vv}}\boldsymbol{H}^H\right) \tag{44}$$

Therefore, the ergodic capacity is obtained by maximizing the expected value of $\mathcal{I}(\boldsymbol{y},\boldsymbol{v}|\boldsymbol{H})$ over all channel realizations

$$\mathrm{C}_o(N_r) = \arg\max_{\text{trace}(R_{\boldsymbol{vv}})=\mathcal{P}} \mathsf{E}_{\mathbf{H}}[\mathcal{I}(\boldsymbol{y},\boldsymbol{v}|\boldsymbol{H})] \tag{45}$$

where $\mathcal{P}$ is the total transmit power and $\mathrm{C}_o(N_r)$ is the original channel capacity also known as the open-loop channel capacity. Substituting $R_{\boldsymbol{vv}} = \mathsf{E}_{\boldsymbol{v}}[\boldsymbol{v}\boldsymbol{v}^H] = \frac{\mathcal{P}}{N_t}\mathbf{I}_{N_t}$ in (44) and taking the expectation with respect to $\boldsymbol{H}$ we get

$$\mathrm{C}_o(N_r) = \mathsf{E}_{\mathbf{H}}\left[\log_2\det\left(\boldsymbol{I}_{N_r}+\frac{\rho}{N_t}\boldsymbol{H}\boldsymbol{H}^H\right)\right] \tag{46}$$

where $\rho = \mathcal{P}/\sigma^2$ is the SNR at each receive antenna. Considering the space-time correlation induced on the channel matrix $\boldsymbol{H}$ by the structure of $\boldsymbol{v}$ in (13), one can obtain the equivalent channel matrix $\boldsymbol{\mathcal{H}}$ given in (14). A new capacity $\mathrm{C}_n(N_r)$ can be computed for the new equivalent channel $\boldsymbol{\mathcal{H}}$ which is different, in general, from the original capacity $\mathrm{C}_o(N_r)$. The difference between the two capacities (if any) i.e. $\boldsymbol{\Delta}\mathrm{C} = \mathrm{C}_o(N_r) - \mathrm{C}_n(N_r)$ quantifies as the information loss due to space-time coding. The capacity of the new equivalent channel $\mathrm{C}_n(N_r)$ is given by [7]

$$\begin{aligned}\mathrm{C}_n(N_r) &= \frac{1}{2}\arg\max \mathsf{E}_{\boldsymbol{\mathcal{H}}}\left[\log_2 \det\left(\mathbf{I}_{2N_r} + \frac{1}{\sigma^2}\boldsymbol{\mathcal{H}}R_{\boldsymbol{ss}}\boldsymbol{\mathcal{H}}^H\right)\right] \\ &\text{subject to} \quad R_{\boldsymbol{ss}} = \frac{\mathcal{P}}{N_t}\boldsymbol{I}_{2N_t} \\ &= \frac{1}{2}\mathsf{E}_{\boldsymbol{\mathcal{H}}}\left[\log_2 \det\left(\boldsymbol{I}_{2N_r} + \frac{\rho}{N_t}\boldsymbol{\mathcal{H}}\boldsymbol{\mathcal{H}}^H\right)\right]\end{aligned} \tag{47}$$

Lemma 1:
Let $\boldsymbol{\Lambda} = \mathrm{diag}(\lambda_1, \lambda_2)$ be the diagonal matrix containing the two non-zero eigenvalues of $\boldsymbol{H}^H\boldsymbol{H}$, which is the Wishart matrix associated with open-loop channel matrix $\boldsymbol{H}$. Then $\boldsymbol{\Lambda}' = \mathrm{diag}(\lambda_1, \lambda_1, \lambda_2, \lambda_2)$ is the diagonal matrix consisting of all 4 non-zero eigenvalues of $\boldsymbol{\mathcal{H}}^H\boldsymbol{\mathcal{H}}$ if and only if

$$a_1^2 + b_1^2 = 1; \quad a_2^2 + b_2^2 = 1; \quad a_1 b_2 - b_1 a_2 = 0 \tag{48}$$

Proof :
Assuming $N_t = 2$ and $N_r \geq 2$, the rank of the $N_r \times N_t$ channel matrix $\boldsymbol{H}$ is 2. Therefore, the non-zero eigenvalues of $\boldsymbol{H}^H\boldsymbol{H}$ are the roots of the characteristic equation

$$\lambda^2 + (c_1 + c_3)\lambda + c_1 c_3 - |c_2|^2 = 0 \tag{49}$$

which can be shown to be the only two eigenvalues of $\boldsymbol{H}^H\boldsymbol{H}$. In (48), we define

$$c_1 = \sum_{i=1}^{N_r} |h_{i1}|^2; \quad c_2 = \sum_{i=1}^{N_r} h_{i1}h_{i2}^*; \quad c_3 = \sum_{i=1}^{N_r} |h_{i2}|^2 \tag{50}$$

When the 3 conditions in (48) are met, it can be easily verified that the characteristic polynomial of the Wishart matrix $\boldsymbol{\mathcal{H}}\boldsymbol{\mathcal{H}}^H$ is of the form

$$\lambda^{2N_r - 4}[\lambda^2 + (c_1 + c_3)\lambda + c_1 c_3 - |c_2|^2]^2 = 0 \tag{51}$$

with $(2N_r - 4)$ zeros and two sets of doubly-repeated eigenvalues; i.e. $\{\lambda_1, \lambda_1\}$ and $\{\lambda_2, \lambda_2\}$. Note that we are considering the case $N_r \geq N_t = 2$. Performing an eigenvalue decomposition of $\boldsymbol{\mathcal{H}}\boldsymbol{\mathcal{H}}^H$ and substituting in (47) we get

$$\begin{aligned}\mathrm{C}_n(N_r) &= \frac{1}{2}\mathsf{E}_{\boldsymbol{\mathcal{H}}}\left[\log_2 \det\left(\boldsymbol{I}_{2N_r} + \frac{\rho}{N_t}\boldsymbol{\mathcal{H}}\boldsymbol{\mathcal{H}}^H\right)\right] \\ &= \frac{1}{2}\log_2 \det\left(\boldsymbol{I}_{2N_r} + \frac{\rho}{N_t}\boldsymbol{\Lambda}'\right) \\ &= \frac{1}{2}\log_2 \prod_{i=1}^{N_t=2}\left(1 + \frac{\rho}{N_t}\lambda_i\right)^2 = \mathrm{C}_o(N_r)\end{aligned} \tag{52}$$

which shows that our MCC code is information lossless for any N_r. Note that the optimum values for design parameters α_i, β_i for $i = 1, 2$ derived for the MTD construction in Section III-A satisfy the conditions in (48) with the ordering given in (12) and, therefore, are used for the MCC construction as well. The price paid is the loss in diversity order of the MCC code which is still acceptable (c.f. Section V) for the low-to-medium SNR range that MIMO wireless links typically operate at and for large signal constellations where the effects of coding gain optimization become more critical on performance.

Appendix C
Proof of Proposition 3

Considering the first user, the equivalent channel $\tilde{\boldsymbol{\mathcal{H}}}$ can be derived as follows

$$\begin{aligned}\tilde{\boldsymbol{\mathcal{H}}} &= \boldsymbol{\mathcal{D}_1}\boldsymbol{\mathcal{H}_1} + \boldsymbol{\mathcal{D}_2}\boldsymbol{\mathcal{Q}_2} \\ &= \boldsymbol{\mathcal{D}_1}\left(\boldsymbol{\mathcal{H}_1} - \boldsymbol{\mathcal{Q}_1}(\boldsymbol{\mathcal{H}_2}^H\boldsymbol{\mathcal{H}_2})^{-1}\boldsymbol{\mathcal{H}_2}^H\boldsymbol{\mathcal{Q}_2}\right)\end{aligned} \tag{53}$$

Permutation of the fourth and the second columns of $\boldsymbol{\mathcal{H}_i}$ or $\boldsymbol{\mathcal{Q}_i}$ in (26) puts these equivalent channel matrices in the form

$$\boldsymbol{\mathcal{H}}_\pi = \begin{bmatrix} \mathcal{A}_1 & \cdots & \mathcal{A}_{N_r} \\ \mathcal{B}_1 & \cdots & \mathcal{B}_{N_r} \end{bmatrix}^t \tag{54}$$

where $\mathcal{A}_i$ and $\mathcal{B}_i$ for $i = 1, \cdots, N_r$ have Alamouti structure. Note that column permutations on the channel matrix correspond to changing the positions of the information symbols and result in an equivalent system of equations. To see if $\tilde{\boldsymbol{\mathcal{H}}}$ has the same structure as $\boldsymbol{\mathcal{H}}$, we note that

$$\boldsymbol{\mathcal{H}}_\pi^H\boldsymbol{\mathcal{H}}_\pi = \begin{bmatrix} \sum_{i=1}^{N_r} \mathcal{A}_i^H\mathcal{A}_i & \sum_{i=1}^{N_r} \mathcal{A}_i\mathcal{B}_i^H \\ \sum_{i=1}^{N_r} \mathcal{A}_i^H\mathcal{B}_i & \sum_{i=1}^{N_r} \mathcal{B}_i^H\mathcal{B}_i \end{bmatrix}_{4\times 4} \tag{55}$$

It can be easily verified that the multiplication of any two Alamouti matrices results in an Alamouti matrix. Therefore, $\boldsymbol{\mathcal{H}}_\pi^H\boldsymbol{\mathcal{H}}_\pi$ is a block Alamouti matrix. Now, to prove Proposition 3, it suffices to prove that the inverse of (55) has block-Alamouti structure since (53) consists only of multiplication and inversion of block-Alamouti matrices.

Lemma 2: *Invariance of block-Alamouti matrices under inversion*:
Consider the block matrix inverse identity

$$\begin{bmatrix} \mathcal{U} & \mathcal{X} \\ \mathcal{T} & \mathcal{W} \end{bmatrix}^{-1} = \begin{bmatrix} \mathcal{U}^{-1} + \mathcal{U}^{-1}\mathcal{X}\mathcal{S}^{-1}\mathcal{T}\mathcal{U}^{-1} & -\mathcal{U}^{-1}\mathcal{X}\mathcal{S}^{-1} \\ -\mathcal{S}^{-1}\mathcal{T}\mathcal{U}^{-1} & \mathcal{S}^{-1} \end{bmatrix} \tag{56}$$

where $\mathcal{S}$ is the Schur complement of $\mathcal{U}$ given by $\mathcal{S} = \mathcal{W} - \mathcal{T}\mathcal{U}^{-1}\mathcal{X}$. Using (56) to evaluate the inverse of (55) and using the fact that

$$\begin{aligned}\mathcal{U}^{-1} &= \left(\sum_{i=1}^{N_r} \mathcal{A}_i^H\mathcal{A}_i\right)^{-1} \\ &= \left(\sum_{i=1}^{N_r} |h_{i1}|^2\alpha_1^2 + \sum_{j=1}^{N_r} |h_{j2}|^2\beta_1^2\right)^{-1} \boldsymbol{I_2}\end{aligned} \tag{57}$$

it can be seen that all the operations in (56) involve block-Alamouti matrix multiplications and inversions which can be shown to have block-Alamouti structure. Therefore, the matrix $(\boldsymbol{\mathcal{H}}_\pi^H\boldsymbol{\mathcal{H}}_\pi)^{-1}$ has block-Alamouti structure and it follows immediately that (53) has block-Alamouti structure. Similarly, it can be shown that

$$\tilde{\boldsymbol{\mathcal{Q}}} = \boldsymbol{\mathcal{D}_4}\left(\boldsymbol{\mathcal{H}_2} - \boldsymbol{\mathcal{Q}_2}(\boldsymbol{\mathcal{H}_1}^H\boldsymbol{\mathcal{H}_1})^{-1}\boldsymbol{\mathcal{H}_1}^H\boldsymbol{\mathcal{Q}_1}\right) \tag{58}$$

has two pairs of columns which are orthogonal to each other. Therefore, we can perform HMLIC for each user separately and achieve the performance of full ML search over all information symbols. The overall multi-user decoder will not be ML-optimal due to the sub-optimality of the first-stage decorrelator. However, its complexity grows only proportional to cq^2 (for c users) compared to a complexity of q^{4c} for the full ML detector resulting in a substantial complexity savings.

REFERENCES

[1] S. M. Alamouti, "A simple transmit diversity technique for wireless communications," *IEEE J. Selected Areas Commun.*, vol. 16, pp. 1451–1458, Oct. 1998.

[2] V. Tarokh, H. Jafarkhani, and A. R. Calderbank, " Space-time block codes from orthogonal designs," *IEEE Trans. Inform. Theory*, vol. 45, pp. 1456–1466, July 1999.

[3] M. O. Damen, A. H. Tewfik, and J. C. Belfiore, "A construction of a spacetime code based on number theory," *IEEE Trans. Inform. Theory*, vol. 48, no. 3, pp. 753–760, Mar. 2002.

[4] P. Dayal and M. K. Varanasi, "An optimal two transmit antenna spacetime code and its stacked extensions," *IEEE Trans. Inform. Theory*, vol. 51, no. 12, pp. 4348–4355, Dec. 2005.

[5] H. Yao and G. W. Wornell, "Achieving the full MIMO diversity-multiplexing frontier with rotation-based space-time codes," in *Proc. Allerton Conference, Communication, Control and Computing*, Monticello, IL, Oct. 2003.

[6] J. C. Belfiore, G. Rekaya, and E. Viterbo, "The Golden Code: a 2×2 full-rate space-time code with nonvanishing determinants," *IEEE Trans. Inform. Theory*, vol. 51, no. 4 pp. 1432–1436, Apr. 2005.

[7] G. D. Golden, G. J. Foschini, R. A. Valenzuela, and P. W. Wolniasky, "Detection algorithm and initial laboratory results using V-BLAST space-time communication architecture," *IEE Electron. Lett.*, vol 35, pp. 14–16, Jan. 1999.

[8] A. Hottinen, O. Tirkkonen, and R. Wichman, *Multi-Antenna Transceiver Techniques for 3G and Beyond*. Wiley, 2003.

[9] J. Paredes, A. B. Gershman, and M. Gharavi-Alkhansari, "A 2×2 space-time code with non-vanishing determinants and fast maximum likelihood decoding," in *Proc. IEEE International Conference on Acoustics, Speech and Signal Processing (ICASSP 2007)*, vol. 2, pp. 877–880, Apr. 2007.

[10] S. Sezginer and H. Sari, "Full-rate full-diversity 2×2 space-time codes of reduced decoder complexity," *IEEE Commun. Lett.*, vol. 11, no. 12, pp. 973–975, Dec. 2007.

[11] K. P. Srinath and B. S. Rajan, "A low-complexity, full-rate, full-diversity 2×2 STBC with Golden code's coding gain," June 2008.

[12] K. P. Srinath and B. S. Rajan, " A low-decoding-complexity, large coding gain, full-rate, full-diversity STBC for 4×2 MIMO system," June 2008.

[13] E. Biglieri, Y. Hong, and E. Viterbo, "On fast-decodable space-time block codes," submitted to *IEEE Trans. Inform. Theory*.

[14] P. Rabiei and N. Al-Dhahir, "A new information lossless STBC for 2 transmit antennas with reduced-complexity ML decoding," in *Proc. IEEE Vehicular Technology Conference (VTC 2007)*, pp. 773–777, Sept. 2007.

[15] P. Rabiei and N. Al-Dhahir, "A new full-rate full-diversity STBC for 2 TX with low complexity ML decoding," in *Proc. IEEE Sarnoff Symposium*, Apr. 2007.

[16] J. Chui and A. R. Calderbank, "Effective coding gain for space-time codes," in *Proc. IEEE International Symposium on Information Theory*, July 2006.

[17] B. Hassibi and B. M. Hochwald, "High-rate codes that are linear in space and time," *IEEE Trans. Inform. Theory*, vol. 48, no. 7, pp. 1804–1824, July 2002.

[18] J. Jaldén and B. Ottersten, "On the complexity of sphere decoding in digital communications," *IEEE Trans. Signal Processing*, vol. 53, no. 4, pp. 1474–1484, Apr. 2005.

[19] N. Al-Dhahir, "Single-carrier frequency-domain equalization for space-time block-coded transmissions over frequency-selective fading channels," *IEEE Commun. Lett.*, vol. 5, no. 7, pp. 304–306, July 2001.

[20] B. L. Hughes, "Differential space-time modulation," *IEEE Trans. Inform. Theory*, vol 46, no. 7, pp. 2567–2578, Nov. 2000.

[21] Y. Zhu and H. Jafarkhani, "Differential modulation based on quasi-orthogonal codes," *IEEE Trans. Wireless Commun.*, vol 4, no. 6, pp. 3018–3030, Nov. 2005.

Payam Rabiei (S'05) received the B.Sc. degree in electrical engineering from Shahid Beheshti University, Tehran, Iran in 2004. Since January 2006, he has been working toward his Ph.D. degree with the department of Electrical Engineering and Computer Science, University of Texas at Dallas. His research interests are space-time coding and processing and low-complexity MIMO receivers. His current research focus is on estimation and compensation of RF impairments in MIMO-OFDM systems.

Author Name Naofal Al-Dhahir earned his MS and Ph.D. degrees from Stanford University in 1990 and 1994, respectively, in Electrical Engineering. He was an Instructor at Stanford University in 1993. From 1994 to 1999, he was a member of the technical staff at GE R&D Center in NY where he worked on satellite communication systems design and anti-jam GPS receivers. From 1999 to 2003, he was a principal member of technical staff at AT&T Shannon Laboratory in NJ where he worked on space-time coding and signal processing. In 2003, he joined UT-Dallas as an Associate Professor and became a full Professor in 2007. His current research interests include broadband wireless transmission, space-time coding and signal processing, MIMO-OFDM transceivers, and digital subscriber line technology. He served as a consultant to several telecommunications companies.

He has authored over 190 journal and conference papers and holds 25 issued US patents. He is a Fellow of the IEEE and a member of the IEEE SP4COM and SPTM technical committees. He served as Editor for IEEE TRANSACTION ON SIGNAL PROCESSING and IEEE COMMUNICATIONS LETTERS and is currently an Editor for IEEE TRANSACTIONS ON COMMUNICATIONS. He served as co-chair of the Communication Theory Symposium at Globecom'04 and Tutorial Co-Chair for ICASSP'08. He is co-author of the book *Doppler Applications for LEO Satellite Systems* (Springer 2002). He is co-recipient of the IEEE VTC Fall 2005 best paper award, the 2005 IEEE signal processing society young author best paper award, and the 2006 IEEE Donald G. Fink best journal paper award.

A.R. Calderbank (M'89-SM'97-F'98) received the BSc degree in 1975 from Warwick University, England, the MSc degree in 1976 from Oxford University, England, and the PhD degree in 1980 from the California Institute of Technology, all in mathematics.

Dr. Calderbank is Professor of Electrical Engineering and Mathematics at Princeton University where he directs the Program in Applied and Computational Mathematics. He joined Bell Telephone Laboratories as a Member of Technical Staff in 1980, and retired from AT&T in 2003 as Vice President of Research. Dr. Calderbank has made significant contributions to a wide range of research areas, from algebraic coding theory and quantum computing to wireless communication and active sensing.

Dr. Calderbank served as Editor in Chief of the IEEE Transactions on Information Theory from 1995 to 1998, and as Associate Editor for Coding Techniques from 1986 to 1989. He was a member of the Board of Governors of the IEEE Information Theory Society from 1991 to 1996 and began a second term in 2006. Dr. Calderbank was honored by the IEEE Information Theory Prize Paper Award in 1995 for his work on the Z4 linearity of Kerdock and Preparata Codes (joint with A.R. Hammons Jr., P.V. Kumar, N.J.A. Sloane, and P. Sole), and again in 1999 for the invention of space-time codes (joint with V.Tarokh and N. Seshadri). He received the 2006 IEEE Donald G. Fink Prize Paper Award and the IEEE Millennium Medal, and was elected to the US National Academy of Engineering in 2005.